Exaggerated in vivo IL-17 responses discriminate recall responses in active TB

Authors

Gabriele Pollara[1*], Carolin T Turner[1], Gillian S Tomlinson[1], Lucy CK Bell[1], Ayesha Khan[1], Luis Felipe Peralta[2], Anna Folino[3], Ayse Akarca[1], Cristina Venturini[1], Tina Baker[1], Fabio LM Ricciardolo[3], Teresa Marafioti[1], Cesar Ugarte-Gil[2,4], David AJ Moore[4,5], Benjamin M Chain[1], Mahdad Noursadeghi[1]

[1] University College London, London, UK

[2] School of Medicine, Universidad Peruana Cayetano Heredia, Lima, Peru

[3] Department of Clinical and Biological Sciences, University of Turin, Turin, Italy

[4] TB Centre, London School of Hygiene & Tropical Medicine, London, UK

[5] Laboratorio de Investigación de Enfermedades Infecciosas, Universidad Peruana Cayetano Heredia, Lima, Peru

Correspondence

Dr Gabriele Pollara – Division of Infection & Immunity, University College London, Gower Street, London, WC1E 6BT. g.pollara@ucl.ac.uk

Running title

IL-17 responses in active TB disease

Manuscript word count

7190 words

Online data

This article has an online data supplement, which includes:

- Supplementary figures S1-7
- Supplementary tables S1-7

Conflict of interest statement

The authors have declared that no conflict of interest exists.

Abstract

Background

Host immune responses at the site of *Mycobacterium tuberculosis* (Mtb) infection serve to contain the pathogen, but also mediate the pathogenesis of tuberculosis (TB) and onward transmission of infection. Based on the premise that active TB disease is predominantly a manifestation of immunopathology, we tested the hypothesis that immune responses at the site of host-pathogen interactions would reveal enrichment of immunopathologic responses in patients with active TB that were absent in individuals with equivalent immune memory for Mtb but without disease.

Methods

In cohorts of patients with active TB and cured or latent infection, we undertook molecular profiling at the site of a tuberculin skin test to model in vivo host-pathogen interactions in Mtb infection. Genome-wide transcriptional differences were identified by differential gene expression analyses. Enrichment of immune cells and cytokine activity was derived using specific transcriptional modules. Findings were validated in independent cohorts of patients with active TB, as well as Mtb infected tissues.

Results

Active TB in humans is associated with exaggerated IL-17A/F expression, accumulation of Th17 cells and IL-17A bioactivity, including increased neutrophil recruitment and matrix metalloproteinase-1 expression directly implicated in TB pathogenesis. These features discriminate recall responses in patients with active TB from those with cured or latent infection, and are also evident at the site of TB disease.

Conclusions

Our data are consistent with a model in which elevated Th17 responses within tissues drive immunopathology and transmission in active TB, and support targeting of the IL-17A/F pathway in host-directed therapy for active TB.

Abstract word count

249 words

Introduction

Mycobacterium tuberculosis (Mtb) infection results in a spectrum of clinical outcomes, from asymptomatic latent infection to symptomatic disease. The focus of host-pathogen interactions is characterised histologically by granuloma formation, a chronic inflammatory process that may contain the infection, but can also result in tissue damage that promotes transmission of infection to other individuals (1, 2). The distinctions that tip the balance between protective and pathogenic immune responses remain a fundamental question in tuberculosis research. This knowledge is expected to inform rational vaccine design and development of host-directed therapies (3).

Chronic inflammatory pathology at the site of human tuberculosis has been the subject of extensive descriptive studies, but discriminating between protective and pathological immune responses has been limited to comparing leucocyte phenotype and function in blood from Mtb-exposed patients with and without active disease (1). We have shown that genome-wide transcriptional profiling of biopsies of the tuberculin skin test (TST) can be used to make comprehensive molecular and systems level assessment of in vivo immune responses at the site of standardised host-pathogen interactions (4–7). Importantly, the transcripts enriched within the TST reflect the genome-wide variation in molecular pathology at the site of tuberculosis (TB) disease (5, 7), suggesting the TST represents a valuable surrogate for assessing TB immunopathogenesis in vivo.

On the premise that active TB disease is predominantly a manifestation of immunopathology, in this study we aimed to test the hypothesis that immune responses at the site of host-pathogen interactions, modelled by the TST, would reveal enrichment of immunopathologic responses in patients with active TB that were absent in individuals with equivalent immune memory for Mtb but without disease.

Results

Immune responses at the site of TST in active and cured TB

The TST has been most extensively used to identify patients with T cell memory for mycobacterial antigens, but the clinical response does not differentiate infected individuals with and without active disease (1). We sought to test the hypothesis that molecular profiling of the TST may identify elements of the recall response which are specifically associated with disease. We undertook 48-hour TSTs in patients with microbiologically-confirmed TB disease within the first month of treatment ('active TB') to identify disease associated responses, and compared these to TST responses in patients within one year of curative TB treatment ('cured TB') to identify non-disease associated recall responses (table

86 S1). Age, gender and site of TB disease were comparable between the two groups (table S2). As
87 expected, clinical induration in response to the TST was not significantly different between the two
88 groups (fig 1A), hitherto interpreted to reflect comparable cell mediated immune memory.

89 In comparison to skin biopsies from the site of control saline injection, 1910 genes were significantly
90 enriched in response to the TST in at least one study group. Of these, 1251 were enriched in both
91 groups (fig 1B). Bioinformatic systems level assessment of the shared response revealed many
92 prototypic cell mediated immune responses which we had previously described in the TST (fig 1C) (5).
93 Pairwise assessment of the integrated list of transcripts that were enriched in either group revealed
94 statistically significant covariance, consistent with the hypothesis that the majority of responses do
95 not discriminate between the two groups (fig 1D).

96 Differential gene expression in the TST in active TB

97 A proportion of genes were differentially enriched between the two groups (fig 1D & tables S3-4). 44
98 genes were expressed significantly more in patients with active TB (table S3) compared to patients
99 with cured TB. Amongst these, pathway analysis identified statistically significant enrichment of
100 transcripts involved in extracellular matrix (ECM) remodelling, such as matrix metalloproteinase 1
101 (MMP-1), and beta defensins that both exert antimicrobial functions and also provide a chemotactic
102 gradient for CCR2-expressing cells, including neutrophils (8) (figs 2A & S1A). MMP-1, previously
103 implicated in pathogenic degradation of the ECM in TB (9), was the most over-expressed gene in
104 active TB compared to cured TB (fig 2B & table S3). This difference was validated at protein level by
105 immunohistochemistry, which also revealed that the differences in MMP-1 expression between
106 patients with active and cured TB was restricted to the inflammatory infiltrates within the TST (fig 2C-
107 E).

108 Elevated IL-17 responses in active TB

109 We hypothesised that the genes over-expressed in active TB were regulated by common upstream
110 signals in the tissue environment. To test this hypothesis, we compared the predicted upstream
111 regulators of differentially expressed transcripts in the TST of active and cured TB patients using
112 Ingenuity Pathway Analysis (6). This analysis suggested that IL-17A induced the expression of genes
113 over-expressed in active TB and not those over-expressed in cured TB (fig 3A). In contrast, IFNγ was
114 predicted to be an upstream signal for gene expression enriched in both active and cured TB (fig 3A).
115 IFNγ responses, largely attributed to T helper (Th)-1 polarised CD4+ T cells are necessary for
116 immunological protection against Mtb (10), but they are insufficient and do not discriminate between
117 people who do and do not develop disease (1). The role of IL-17A in TB is less clear. This cytokine

118 belongs to a family of six structurally related cytokines and shares greatest sequence homology with
119 IL-17F. These bind the same receptor, and consequently exert the same functions, particularly
120 increased neutrophil recruitment via upregulation of chemokine expression (11).

121 There is unequivocal evidence that IL-17A/F contribute to host defence against bacterial and fungal
122 pathogens (12). Importantly however, they are also strongly indicated in the immunopathology of
123 chronic inflammatory diseases (12, 13). This includes evidence for IL-17A dependent neutrophil
124 mediated pathology in mouse models of Mtb infection (14–16). Our bioinformatics analysis suggested
125 increased enrichment of transcripts in the human in vivo recall response of patients with active TB
126 may be driven by IL-17A/F activity. Therefore, we sought to test the hypothesis that IL-17A/F activity
127 is exaggerated in active TB. Consistent with this hypothesis the expression of both IL-17A and IL-17F
128 were enriched in the TST of people with active TB compared to cured TB (fig 3B). In contrast, IFNγ
129 transcript levels representing the prototypic molecule in cell mediated immune recall responses was
130 not significantly different (fig 3B). Interestingly, the expression of IL-22, a cytokine with closely related
131 biological function to IL-17A and IL-17F (17), was also not elevated in active TB (fig 3B). The differences
132 revealed at the transcriptional level were also reflected by increased immunofluorescence of IL-17F
133 protein in the TST of people with active TB (fig 3C & 3D).

134 In order to test the functional significance of the differences in IL-17A/F expression between active
135 and cured TB, we evaluated differences in the bioactivity of IL-17A between these groups. We
136 addressed this by generating cellular response modules from the transcriptomes of
137 cytokine-stimulated keratinocytes (KC) (18, 19). We confirmed that these modules were both sensitive
138 and specific for their cognate stimuli by assessing their expression in other independent datasets (fig
139 S2). We then compared the geometric mean expression of these cytokine-specific transcriptional
140 modules in the TST transcriptomes. The IL-17A-induced gene module was significantly increased in the
141 TST of people with active TB compared to that of cured TB, but expression of IFNγ, type I IFN or
142 TNF-inducible gene modules was not significantly different between the two groups (fig 4A). We
143 extended our approach to evaluating the functional bioactivity of other specific cytokines using
144 transcriptional modules for IL-10- and IL-4/IL-13-inducible gene expression, described in a previous
145 report (5). Neither of these were significantly different in the TST of people with active and cured TB
146 (fig S3A). The IL-4/IL-13 bioactivity module was used as a measure of Th2 responses normally
147 associated with allergy and immune responses to helminths. Another member of the IL-17 family, IL-
148 17E contributes to Th2 responses (11). We found no enrichment of IL-17E expression in the TST of
149 people with active TB consistent with IL-4/IL-13 bioactivity and distinct from IL-17A/F bioactivity (fig
150 S3B).

151 Focusing on mechanisms that may contribute to pathogenesis, enrichment of MMP-1 expression in
152 the TST of patients with active TB (fig 2) can also be attributed to increased IL-17A/F bioactivity,
153 through induction of MMP expression by stromal cells (20). Neutrophils can also contribute to the
154 immunopathology of TB (14–16, 21, 22), and a key function of IL-17A/F is to promote neutrophil
155 recruitment via induction of neutrophil chemokines (12). Therefore, we tested the hypothesis that the
156 TST in active TB will also reveal increased neutrophil recruitment, compared to that of patients with
157 cured TB. We compared the expression of two independently derived transcriptional modules that
158 have been extensively validated to reflect neutrophil frequency in tissues including the TST (23, 24).
159 We found significantly higher expression of the neutrophil modules in people with active TB compared
160 to cured TB (fig 4B). These differences were mirrored by gene expression levels of IL-17A-inducible
161 CXCL1, CXCL8 and S100A9 that drive neutrophil recruitment to sites of inflammation (11, 15) (fig 4C).
162 In contrast, accumulation of monocytes and T cells assessed by their respective gene expression
163 modules (23), and the expression of the monocyte chemoattractant, CCL2, did not differ in the TST of
164 people with active and cured TB (fig 4B&C).

165 Increased frequency of Th17 cells in active TB TST responses

166 IL-17A/F are predominantly produced by Th17 cells and neutrophils (11). Immunohistochemistry
167 revealed that in the TST of people with active TB, IL-17F, originated predominantly from mononuclear
168 cells, rather than from polymorphonuclear cells (fig 5A). Therefore, we tested the hypothesis that
169 Th17 cells were enriched in the TST of people with active TB compared to that of cured TB. We derived
170 transcriptional modules specific for differentially polarised CD4+ Th subsets from a published dataset
171 (25) and demonstrated their specificity in an independent dataset (26) (fig S4A). We further validated
172 the Th17 module by showing that this correlated closely with the expression of the IL-17A/F bioactivity
173 module within skin biopsies of patients with psoriasis vulgaris, representing an alternative Th17-
174 mediated inflammatory condition (27) (fig S4B). The expression of the Th1- and Th2-associated
175 transcriptional modules in the TST was comparable between patients with active and cured TB, but
176 expression of the Th17 associated module was significantly increased in patients with active TB (figs
177 5B & S3).

178 In order to investigate the mechanism for increased Th17 responses in the TST of patients with active
179 TB, we tested the hypothesis that active TB was also associated with increased circulating Th17 cells.
180 We assessed the expression of the Th subset modules in the transcriptome of PPD-stimulated PBMC
181 from an independent cohort of individuals with active TB disease and latent TB infection (28). In
182 contrast to that observed in the TST, patients with active TB revealed enrichment for the
183 Th1-associated gene expression module in PBMC but showed no difference in the Th17-associated

184 module (fig 5C). As a result, we explored the alternative hypothesis that the inflammatory
185 environment generated at the site of TST promotes the Th17 differentiation observed in patients with
186 active TB. We investigated the expression of cytokines implicated in Th17 differentiation, IL-1β, IL-6,
187 IL-23 and TGFβ (11). The expression of each of these was significantly correlated with enrichment for
188 Th17 cells in the TST of active TB. In contrast there was no correlation with IL-12 and IL-4 expression
189 that drive Th1 and Th2 cell differentiation respectively (fig 5D). These data support a model in which
190 the local tissue microenvironment may promote Th17 differentiation within tissues in active TB.

191 IL-17 activity is not a feature of latent TB and is not confounded by demographic background, 192 extrapulmonary disease or time on treatment

193 In order to validate our findings, we compared the TST transcriptome of a second independent cohort
194 of people with active TB with that of individuals with latent TB infection. Consistent with our previous
195 results, this comparison revealed significant enrichment for IL-17A/F bioactivity and neutrophil
196 infiltration in people with active TB (fig 6A). Furthermore, Th17 cells were enriched in those with active
197 TB despite there being no overall difference in T cell numbers compared to the TST in individuals with
198 latent TB (fig 6A). Of note, the comparison to latent TB in this analysis, also excluded the possibility
199 that lower levels of IL-17A/F bioactivity in the TST of people with cured TB compared to active TB was
200 an off-target effect of the antimicrobial treatment for active TB.

201 Taken together our data show that active TB is associated with exaggerated Th17 recall responses and
202 IL-17 bioactivity within the tissue microenvironment of host-pathogen interactions. Our findings were
203 replicated using two different methods for transcriptional profiling (microarray figs 4-5 and RNA-Seq
204 fig 6), and were consistent in geographically distinct cohorts (fig S5A). Significantly exaggerated Th17
205 recall and IL-17A/F bioactivity in people with active TB compared to either cured or latent TB were
206 preserved in analyses including only UK cohorts (figs S5B & S5C), confirming that the differences were
207 not due to confounding by other variables in the different cohorts. In addition, we found no difference
208 in these responses between people with pulmonary and extrapulmonary TB disease (fig S6). Of note,
209 people with active TB were assessed at different time points within the first month of treatment
210 (median 11 days, IQR 5-28 days). Rapid changes in the peripheral blood transcriptome associated with
211 active TB have been reported (29, 30), but we found no diminution of the exaggerated Th17 recall
212 responses and IL-17A bioactivity invoked by the TST challenge in this time frame (fig S7), suggesting
213 that the mechanisms that drive these responses in active are not swiftly reversed by treatment.

214 IL-17 activity is present at the site of TB disease

215 Having established that IL-17A/F production by T cells was a prominent feature of the in vivo tissue
216 recall response to Mtb stimulation, we sought to determine whether this was also evident at the site
217 of TB disease. The transcriptome of human TB granuloma (31) showed an enrichment of T cells, Th17
218 cells and IL-17A bioactivity compared to normal lung tissue (fig 6B). In addition, we examined the
219 transcriptome of human Mtb-infected lymphadenitis compared to other 'reactive' causes of
220 lymphadenopathy devoid of granulomatous inflammation or malignancy (32). Interestingly, despite
221 the fact that reactive lymph nodes were enriched for the T cell transcriptional module, the Th17 and
222 IL-17A/F bioactivity modules were enriched within Mtb infected lymph nodes (fig 6C), further
223 confirming enrichment for IL-17A/F bioactivity to be a feature at the site of TB disease.

224 Discussion

225 Active TB disease is characterised by chronic inflammation that can result in significant tissue
226 destruction, necessary for the onward transmission of Mtb (2). Identifying the processes that govern
227 this immunopathology offers the opportunity to intervene therapeutically, limiting tissue damage and
228 transmission of infection. Pathogenic immune pathways have been difficult to identify because most
229 components of the immune response to Mtb do not discriminate between different clinical outcomes
230 of infection (1). The present study provides compelling new evidence that IL-17A/F responses may
231 mediate immunopathology in active TB. The inclusion of multiple cohorts and diverse demographic
232 backgrounds increased the generalisability of our findings and circumvented the limitations of our
233 cross-sectional study design. The findings are consistent with the well-established role of IL-17A/F in
234 the immunopathology of chronic inflammatory human disease exemplified by psoriasis, for which
235 blockade of the IL-17A/F axis provides an effective treatment (13).

236 Importantly, the primary physiological role of IL-17A/F is to promote host defence against bacterial
237 and fungal infection, cogently demonstrated by mice deficient for IL-17A/F or IL-17 receptors, and by
238 humans with inborn errors of IL-17 immunity (12). Mouse models also suggest a protective role for IL-
239 17A/F following BCG vaccination (33) and in the early stages of Mtb infection, particularly in the
240 context of more virulent Mtb strains (34, 35), through localising T cells near Mtb-infected
241 macrophages (34) and by preventing formation of necrotic granuloma (36). However, in mice
242 rendered susceptible to TB disease as a result of IFNγ deficiency or through receiving repeated BCG
243 vaccinations, IL-17A/F responses drive neutrophil-mediated pathology (14–16, 21). We infer from
244 these data that IL-17A/F responses may play a dichotomous role in TB by contributing to protection in
245 early infection, but to the pathology of disease if early infection is not controlled and multibacillary
246 bacterial replication and chronic immune activation ensues. Additional support for this model is
247 evident in IL-27R deficient mice, which exhibit exaggerated Th17 responses because they lack IL-27

248 inhibition of RORγT (37). These mice show enhanced clearance of Mtb, but also increased
249 immunopathology dependent on IL-17A. Interestingly, a human candidate gene study identified host
250 genetic variation associated with increased secretion of IL-17A to be correlated with both protection
251 from incident TB but also more severe TB disease (38). Taken together, we hypothesise that
252 exaggerated IL-17A/F recall responses are the consequence of chronic multibacillary infection, but in
253 turn mediate increased pathology in established disease. Of the other IL-17 family members that signal
254 via alternative receptors, much less is known about the functional role of IL-17B, IL-17C and IL-17D
255 (11). These cytokine responses were not specifically tested in the present study. IL-17E, known to
256 promote Th2 responses (11), was not differentially enriched in active TB. Equally, we found no
257 evidence of elevated IL-10 responses in active TB, indicating an uncoupling of IL-17A/F activity from
258 regulatory responses, driving immunopathology rather than the control of Mtb replication (39).
259 Another cytokine, IL-22, does have functional overlap with IL-17A/F (17), but did not discriminate
260 between people with and without disease in our study.

261 Our data support the hypothesis that exaggerated IL-17A/F responses arise from Th17 cells, but they
262 do not unequivocally exclude other cellular sources. Our immunohistochemical analysis did not show
263 any clear evidence for IL-17F production by polymorphonuclear cells in the TST, but we were not able
264 to test whether other lymphocyte populations, such as γδ T cells, made a significant contribution (35,
265 40, 41). Future studies will require single cell resolution to definitively confirm the source of
266 exaggerated IL-17A/F responses in this model, as well as to determine whether active TB shows
267 enrichment for 'pathogenic' Th17 cells that express both IFNg and IL-17A/F (42). Consistent with
268 previous studies (40, 43), we found no evidence of increased circulating Th17 cells in active TB,
269 although this was measured in a separate active TB cohort to the ones that underwent TST
270 assessment. Nevertheless, this observation underscores the unique value of molecular level
271 assessment of immune responses in the tissue microenvironment at the site of host-pathogen
272 interactions, modelled by the TST. Importantly, it also suggests the model that differential Th17
273 responses within the TST are governed by immune signalling networks within the tissue
274 microenvironment after T cell recruitment. In active TB patients, the tissue expression of cytokines
275 that promote Th17 differentiation correlated with the transcriptional module for Th17 cells. The
276 source of these cytokines is likely to be myeloid cells (11, 13, 44). Although we cannot prove a causal
277 relationship at this stage, our data are consistent with a model in which infiltrating monocytes from
278 patients with active TB secrete elevated levels of cytokines that promote the differentiation of
279 recruited T cells to a Th17 phenotype. Of note, active TB patients have higher frequency of circulating
280 CD14+ CD16+ non-classical monocytes (45), which can potentiate the differentiation of CD4 T cells to
281 a Th17 phenotype in patients with chronic inflammatory conditions (46).

282 Our findings challenge the long-established view that curative treatment of TB does not lead to
283 contemporaneous changes to immunological recall responses (47). Our data are consistent with the
284 hypothesis that IL-17A-inducible neutrophil chemotaxis and expression of MMP-1 represent key
285 mediators of immunopathology in TB by promoting granuloma formation, bacterial replication and
286 matrix degradation that can lead to cavitation and onward transmission (9, 48). Our results support
287 future studies to evaluate the impact of modulating IL-17A/F activity to ameliorate the pathology
288 associated with chronic TB disease. The availability of therapies that block the IL-17A/F cytokine axis,
289 developed and licensed for chronic inflammatory diseases (13), offers invaluable opportunities to
290 transition from proof of concept pre-clinical studies, for example in non-human primate models, to
291 first in man experiments.

292

293 Methods

294 Study populations

295 The study comprised recruitment of several different populations. The discovery 'Active TB' group that
296 formed the basis of most of the analyses in figs 1-5 was the HIV seronegative patients from the same
297 cohort described in our previous publication (5), who were recruited from TB clinics in London, UK and
298 Cape Town, South Africa, and were all within one month of commencing antibiotic therapy. The
299 comparator 'Cured TB' group was an independent cohort recruited from TB clinics in London, UK and
300 Lima, Peru who fulfilled the inclusion/exclusion criteria (table S1). All 'Cured TB' patients were less
301 than 2 years after completion of curative anti-TB antibiotic therapy for drug sensitive disease. In
302 addition, a separate validation cohort of patients with active TB was recruited from TB clinics in
303 London (fig 6). These patients were also within one month of commencing antibiotic therapy. This
304 population was compared to individuals with latent TB recruited from TB clinics in London and Lima,
305 who fulfilled inclusion/exclusion criteria (table S1). All study participants were HIV seronegative and
306 for those with active or cured TB, the presence of Mtb infection was confirmed by routine culture or
307 molecular based methods according to local clinic protocols. The demographic, clinical and laboratory
308 data for each study group is summarised in table S2.

309

310 Study approval

311 Recruitment of patients with cured and latent TB was approved by UK National Research Ethics
312 Committee (reference number: 14/LO/0505) and Universidad Peruana Cayetano Heredia Institutional

313 Ethics Committee (reference number: 62349). Recruitment of patients for the validation active TB
314 cohort was approved UK National Research Ethics Committee (reference number: 16/LO/0776).
315

316 Study schedule and sampling

317 On recruitment to the study, all participants received 0.1 mL intradermal injection of two units
318 tuberculin (Serum Statens Institute) or saline in the volar aspect of one forearm, and this site was
319 marked with indelible ink. At 48 hours, the clinical response at the injection site was evaluated by
320 measurement of the maximum diameter of inflammatory induration and two 3 mm adjacent punch
321 biopsies were obtained from marked TST or saline injection site as previously described (4). One biopsy
322 was placed in RNAlater (Thermo Fisher) and stored at -70°C, and the other biopsy was placed in 10%
323 formalin neutral buffered solution (Sigma-Aldrich) and stored at room temperature for at least 1 week
324 prior to paraffin embedding.
325

326 Sample processing

327 The TST transcriptome from active TB patients in the discovery cohort was derived directly from the
328 data repository E-MTAB-3254 (ArrayExpress - https://www.ebi.ac.uk/arrayexpress/). Skin samples
329 from all other participants was stored in RNAlater at -70oC after collection. For processing, TST
330 samples were equilibrated to room temperature for 30 minutes before being transferred to CK14
331 lysing kit tubes (Bertin Instruments) containing 350µl of Buffer RLT (Qiagen) supplemented with 1% 2-
332 Mercaptoethanol (Sigma). Tubes were pulsed for 6 cycles on a Precellys Evolution homogeniser (Bertin
333 Instruments), each cycle consisting of 23 seconds of homogenisation at speeds of 6300 rpm. Samples
334 were rested on ice for 2 minutes between cycles. After homogenisation, cellular debris and lysing
335 beads were precipitated by centrifugation and RNA isolated from the supernatant using RNeasy Mini
336 Kit (Qiagen). Total RNA from TST samples of patients with cured TB was purified, labelled and
337 hybridised on Agilent 8x60k microarrays as previously described (5). For the validation cohort of active
338 TB and individuals with latent TB, the KAPA mRNA HyperPrep Kit (Roche Diagnostics) was used to
339 construct stranded mRNA-Seq libraries from up to 500 ng intact total RNA after which paired-end
340 sequencing was carried out using the 75 cycle high-output kit on the NextSeq 500 desktop sequencer
341 (Illumina). Each run contained 24 samples and was demultiplexed using bcl2fastq by Illumina
342 (https://support.illumina.com/sequencing/sequencing_software/bcl2fastq-conversion-
343 software.html). Paired end reads were mapped to the Ensembl human transcriptome reference
344 sequence (homo sapiens GRCh38, latest version available). Mapping and generation of read counts

345 per transcript were done using Kallisto (49). R/Bioconductor package tximport was used to import the
346 mapped counts data and summarise the transcripts-level data into gene level (50).
347

348 ## Whole genome transcriptional profiling and analysis software

349 Raw microarray data was processed and normalised as previously described (51). Raw RNASeq counts
350 were normalised within-sample into TPM (transcripts per million) to remove feature-length and
351 library-size effects (52). Log2 transformed TPM were used for further analysis. Data matrices from
352 non-TST datasets were obtained from processed data series downloaded at the ArrayExpress
353 repository. Probe identifiers were converted to gene symbols using platform annotations provided
354 with each dataset. In circumstances where downloaded datasets were not log2 transformed, this was
355 performed on the entire processed data matrix. Significant gene expression differences between
356 datasets were calculated from normalised expression matrices using MultiExperiment Viewer v4.9
357 (http://www.tm4.org/mev.html). Pathway analysis was performed in InnateDB (53) and visualized as
358 network diagrams in Gephi v0.8.2 beta. Upstream regulator analysis was performed using Ingenuity
359 Pathway Analysis (Qiagen), focusing on cytokines with predicted activation z-score >2. Genes
360 predicted to be regulated in either active or cured TB formed the basis of the network diagram in fig
361 3. The expression of transcriptional modules was determined by calculating the geometric mean
362 expression of all the module constituent genes found in the dataset being analysed, using R scripts
363 generated in our previous publication (23), and which are available to download and use from the
364 Github repository (https://github.com/MJMurray1/MDIScoring). Venn diagrams were constructed
365 using the BioVenn tool (http://www.biovenn.nl/).

366

367 ## Transcriptomic data repositories

368 All transcriptional datasets used in this study are described in table S5. Accession numbers refer to
369 datasets in the ArrayExpress repository (https://www.ebi.ac.uk/arrayexpress/). The TST
370 transcriptome of the discovery cohort of patients with active TB was derived from dataset E-MTAB-
371 3254, the cured TB TST transcriptome was derived from dataset E-MTAB-6815, and the validation
372 active TB and latent TB TST transcriptomes were derived from dataset E-MTAB-6816.

373 ## Module derivation and expression

374 Immune cell modules used were ones rated with the highest Module Discriminatory Index (MDI) score
375 for module sensitivity and specificity as determined in our previous publication (23). These were

376 “M19” (T cells), “M37.1” (neutrophils) and “Monocyte 2-fold” (monocytes). We also made use of
377 another neutrophil module “ImSig” that was derived and validated elsewhere (24). We have
378 previously generated and validated the specificity of macrophage response modules to IL-10 or IL4/IL-
379 13 stimulation (5), and these are also utilised in this manuscript.

380 To derive keratinocyte (KC) cytokine-response modules, we made use of previously published
381 transcriptomic data (GSE12109 & GSE36287) from primary human keratinocytes (KCs) stimulated with
382 a selection of cytokines (18, 19). Significant transcriptional responses (paired t-test with α of $p<0.05$
383 and no multiple testing correction) of genes over-expressed >4-fold in the cognate cytokine condition
384 relative to unstimulated KC were initially identified. Modules were then derived from genes that were
385 not also upregulated > 2-fold by non-cognate cytokine conditions compared to unstimulated KC. The
386 KC IL-17 response module utilised a cut-off of 2-fold between IL-17 stimulated KC and unstimulated
387 KC as too few genes were upregulated >4-fold compared to unstimulated KC. The constituent genes
388 of the KC modules are shown in table S6. The KC TNFa response module generated in this way has
389 already been published (6), but the other cytokine modules are newly described. The gene
390 components of the KC cytokine-response modules are available in table S6, and their specificity was
391 evaluated in both datasets in which they were derived and in independent datasets of in vitro
392 cytokine-stimulated KC (fig S1A).

393 The transcriptome of CD4+ T cells polarised towards different T helper phenotypes was derived from
394 dataset GSE54627 (25). To derive specific modules for each differentiation state, we used gene
395 expression from cells stimulated with anti-CD3 and anti-CD28, identifying genes over-expressed in the
396 phenotype of interest compared to all other conditions by paired t-test with α of $p<0.05$ and no
397 multiple testing correction. Each module was derived from the unique genes over expressed by more
398 than 1.5-fold in the cognate condition compared to all other stimulation conditions (except for Th1
399 module where a 2 -fold cut-off was used). The gene components of T helper modules are available in
400 table S7, and their specificity was evaluated in the dataset from which they were derived, in an
401 independent dataset of polarised CD4 T cells, and in skin biopsies of patients with psoriasis vulgaris
402 (fig S1B) (25–27).

403

404 ## Immunostaining

405 Immunostaining of IL-17F was performed on 10 μm sections as previously described (54). Briefly,
406 monoclonal mouse-anti-IL-17F, 1:50, code MA5-16229 [Thermo Fisher Scientific, Waltham, MA, USA]
407 and DAPI (sc-24941, Santa Cruz Biotechnology, Texas, Dallas, USA) for detecting nuclei were used.

408 Irrelevant primary antibodies from Sigma (Milan, Italy; irrelevant mouse, 1:50, code I8765) were
409 applied at the same concentration of the related specific primary antibodies for immunostaining of
410 negative control slides, and as a further negative control, secondary antibody (AF568, goat anti-
411 mouse; Invitrogen, Thermo Fisher Scientific, Waltham, MA, USA) alone was used (data not shown).
412 Light-microscopic analysis was performed at a magnification of 40x with a Leica DM4000B microscope
413 equipped with DFC-320 Leica digital camera (Leica Microsystems, Wetzlar, Germany). Zeiss confocal
414 microscope (LSM800, Carl Zeiss, Germany) was used to acquire confocal images. Quantification of IL-
415 17F was performed on 10x confocal images of samples through the measurement of mean grey value
416 (MGV) using software ImageJ (https://imagej.net/Fiji).

417 Immunostaining of MMP-1 was performed as previously described (55, 56). Scanned slide images
418 were obtained with use of NanoZoomer Digital Pathology System (Hamamatsu, Japan. Quantification
419 of MMP-1 staining was performed blindly by extracting MMP-1 associated 3, 3 -diaminobenzidine
420 (DAB) stain using standard deconvolution protocols in ImageJ. Cellular infiltrates were manually
421 selected as depicted in Fig 2 and DAB stain quantified by staining intensity as proportion of the area
422 selected using ImageJ. The selected region was moved without resizing to adjacent tissue that did not
423 contain cellular infiltration to calculate background MMP-1 intensity. Three cellular infiltrates and
424 background tissue regions were analysed for each tissue samples. Six TST samples were quantified in
425 each group.

426 ## Author contributions

Substantial contributions to the conception or design of the work;	GP, CT, GST, LCB LFP, TM, CU, DAM, BMC, MN
Substantial contributions to the acquisition, analysis, or interpretation of data for the work;	GP, CT, GST, LCB, AK, LFP, AF, AA, CV, TB, FLR, TM, BMC, MN
Drafting the work or revising it critically for important intellectual content;	GP, CT, GST, LCB, BMC, MN
Final approval of the version submitted for publication	All authors
Accountability for all aspects of the work in ensuring that questions related to the accuracy or integrity of any part of the work are appropriately investigated and resolved	GP, MN

427

428

429 ## Acknowledgements

430 The work presented in this manuscript received funding from the Wellcome Trust (WT101766/Z/13/Z
431 to GP and 207511/Z/17/Z to MN), Medical Research Council (MR_N007727_1 to GST) and National
432 Institute for Health Research Biomedical Research Centre at University College London Hospitals.

433 We thank our team of research nurses, in particular Cristina F Turienzo and Victoria Dean, for their
434 assistance in recruiting patients and collecting samples, and the UCL-UCLH Pathogen Genomics Unit
435 for RNASeq sample processing (https://www.ucl.ac.uk/infection-immunity/pathogen-genomics-unit).

436 ## References

437 1. O'Garra A et al. The Immune Response in Tuberculosis. *Annu. Rev. Immunol.* 2013;31(1):475–527.

438 2. Elkington PT, Ugarte-Gil CA, Friedland JS. Matrix metalloproteinases in tuberculosis. *Eur. Respir. J.*
439 2011;38(2):456–464.

440 3. Tiberi S et al. Tuberculosis: progress and advances in development of new drugs, treatment
441 regimens, and host-directed therapies. *Lancet Infect. Dis.* 2018;18(7):e183–e198.

442 4. Tomlinson GS et al. Transcriptional profiling of innate and adaptive human immune responses to
443 mycobacteria in the tuberculin skin test. *Eur. J. Immunol.* 2011;41(11):3253–3260.

444 5. Bell LCK et al. In Vivo Molecular Dissection of the Effects of HIV-1 in Active Tuberculosis. *PLOS Pathog*
445 2016;12(3):e1005469.

446 6. Byng-Maddick R et al. Tumor Necrosis Factor (TNF) Bioactivity at the Site of an Acute Cell-Mediated
447 Immune Response Is Preserved in Rheumatoid Arthritis Patients Responding to Anti-TNF Therapy.
448 *Front. Immunol.* 2017;8:932.

449 7. Lachmandas E et al. Tissue Metabolic Changes Drive Cytokine Responses to Mycobacterium
450 tuberculosis [Internet]. *J. Infect. Dis.* [published online ahead of print: 2018]; doi:10.1093/infdis/jiy173

451 8. Röhrl J, Yang D, Oppenheim JJ, Hehlgans T. Human β-Defensin 2 and 3 and Their Mouse Orthologs
452 Induce Chemotaxis through Interaction with CCR2. *J. Immunol.* 2010;184(12):6688–6694.

453 9. Elkington P et al. MMP-1 drives immunopathology in human tuberculosis and transgenic mice. *J.*
454 *Clin. Invest.* 2011;121(5):1827–1833.

455 10. Jouanguy E et al. Partial interferon-gamma receptor 1 deficiency in a child with tuberculoid bacillus
456 Calmette-Guérin infection and a sibling with clinical tuberculosis.. *J. Clin. Invest.* 1997;100(11):2658–
457 2664.

458 11. Iwakura Y, Ishigame H, Saijo S, Nakae S. Functional Specialization of Interleukin-17 Family
459 Members. *Immunity* 2011;34(2):149–162.

460 12. Li J, Casanova J-L, Puel A. Mucocutaneous IL-17 immunity in mice and humans: host defense vs.
461 excessive inflammation. *Mucosal Immunol.* 2018;11(3):581–589.

462 13. Hawkes JE, Chan TC, Krueger JG. Psoriasis pathogenesis and the development of novel targeted
463 immune therapies. *J. Allergy Clin. Immunol.* 2017;140(3):645–653.

464 14. Cruz A et al. Pathological role of interleukin 17 in mice subjected to repeated BCG vaccination after
465 infection with Mycobacterium tuberculosis. *J. Exp. Med.* 2010;207(8):1609–1616.

466 15. Gopal R et al. S100A8/A9 Proteins Mediate Neutrophilic Inflammation and Lung Pathology during
467 Tuberculosis. *Am. J. Respir. Crit. Care Med.* 2013;188(9):1137–1146.

468 16. Desvignes L, Ernst JD. Interferon-γ-Responsive Nonhematopoietic Cells Regulate the Immune
469 Response to Mycobacterium tuberculosis. *Immunity* 2009;31(6):974–985.

470 17. Ronacher K, Sinha R, Cestari M. IL-22: An Underestimated Player in Natural Resistance to
471 Tuberculosis? [Internet]. *Front. Immunol.* 2018;9. doi:10.3389/fimmu.2018.02209

472 18. Nograles KE et al. Th17 cytokines interleukin (IL)-17 and IL-22 modulate distinct inflammatory and
473 keratinocyte-response pathways. *Br. J. Dermatol.* 2008;159(5):1092–1102.

474 19. Swindell WR et al. Heterogeneity of Inflammatory and Cytokine Networks in Chronic Plaque
475 Psoriasis. *PLOS ONE* 2012;7(3):e34594.

476 20. Singh S et al. Interleukin-17 regulates matrix metalloproteinase activity in human pulmonary
477 tuberculosis. *J. Pathol.* 2018;244(3):311–322.

478 21. Nandi B, Behar SM. Regulation of neutrophils by interferon-γ limits lung inflammation during
479 tuberculosis infection., Regulation of neutrophils by interferon-γ limits lung inflammation during
480 tuberculosis infection. *J. Exp. Med. J. Exp. Med.* 2011;208, 208(11, 11):2251, 2251–2262.

481 22. Marais S et al. Neutrophil-Associated Central Nervous System Inflammation in Tuberculous
482 Meningitis Immune Reconstitution Inflammatory Syndrome. *Clin. Infect. Dis.* 2014;59(11):1638–1647.

483 23. Pollara G et al. Validation of Immune Cell Modules in Multicellular Transcriptomic Data. *PLOS ONE*
484 2017;12(1):e0169271.

485 24. Nirmal AJ et al. Immune Cell Gene Signatures for Profiling the Microenvironment of Solid Tumors.
486 *Cancer Immunol. Res.* 2018;6(11):1388–1400.

487 25. Touzot M et al. Combinatorial flexibility of cytokine function during human T helper cell
488 differentiation [Internet]. *Nat. Commun.* 2014;5. doi:10.1038/ncomms4987

489 26. Ramesh R et al. Pro-inflammatory human Th17 cells selectively express P-glycoprotein and are
490 refractory to glucocorticoids. *J. Exp. Med.* 2014;211(1):89–104.

491 27. Russell CB et al. Gene expression profiles normalized in psoriatic skin by treatment with
492 brodalumab, a human anti-IL-17 receptor monoclonal antibody.. *J. Immunol. Baltim. Md 1950*
493 2014;192(8):3828–3836.

494 28. Lu C et al. Novel Biomarkers Distinguishing Active Tuberculosis from Latent Infection Identified by
495 Gene Expression Profile of Peripheral Blood Mononuclear Cells. *PLoS ONE* 2011;6(8):e24290.

496 29. Bloom CI et al. Detectable changes in the blood transcriptome are present after two weeks of
497 antituberculosis therapy. *PloS One* 2012;7(10):e46191.

498 30. Cliff JM et al. Distinct Phases of Blood Gene Expression Pattern Through Tuberculosis Treatment
499 Reflect Modulation of the Humoral Immune Response. *J. Infect. Dis.* 2013;207(1):18–29.

500 31. Kim M-J et al. Caseation of human tuberculosis granulomas correlates with elevated host lipid
501 metabolism. *EMBO Mol. Med.* 2010;2(7):258–274.

502 32. Tomlinson GS et al. Transcriptional Profiling of Endobronchial Ultrasound-Guided Lymph Node
503 Samples Aids Diagnosis of Mediastinal Lymphadenopathy. *CHEST* 2016;149(2):535–544.

504 33. Khader SA et al. IL-23 and IL-17 in the establishment of protective pulmonary CD4+ T cell responses
505 after vaccination and during Mycobacterium tuberculosis challenge. *Nat. Immunol.* 2007;8(4):369–
506 377.

507 34. Gopal R et al. Unexpected Role for IL-17 in Protective Immunity against Hypervirulent
508 Mycobacterium tuberculosis HN878 Infection. *PLoS Pathog.* 2014;10(5):e1004099.

509 35. Yoshida YO et al. Essential Role of IL-17A in the Formation of a Mycobacterial Infection-Induced
510 Granuloma in the Lung. *J. Immunol.* 2010;184(8):4414–4422.

511 36. Domingo-Gonzalez R et al. Interleukin-17 limits hypoxia-inducible factor 1**α** and development of
512 hypoxic granulomas during tuberculosis [Internet]. *JCI Insight* 2017;2(19).
513 doi:10.1172/jci.insight.92973

514 37. Erdmann H et al. The increased protection and pathology in Mycobacterium tuberculosis -infected
515 IL-27R-alpha-deficient mice is supported by IL-17A and is associated with the IL-17A-induced
516 expansion of multifunctional T cells. *Mucosal Immunol.* 2018;11(4):1168–1180.

517 38. Rolandelli A et al. The IL-17A rs2275913 single nucleotide polymorphism is associated with
518 protection to tuberculosis but related to higher disease severity in Argentina. *Sci. Rep.* 2017;7:40666.

519 39. Gideon HP et al. Variability in Tuberculosis Granuloma T Cell Responses Exists, but a Balance of
520 Pro- and Anti-inflammatory Cytokines Is Associated with Sterilization. *PLOS Pathog*
521 2015;11(1):e1004603.

522 40. Coulter F et al. IL-17 Production from T Helper 17, Mucosal-Associated Invariant T, and γδ Cells in
523 Tuberculosis Infection and Disease. *Front. Immunol.* 2017;8:1252.

524 41. Lockhart E, Green AM, Flynn JL. IL-17 production is dominated by gammadelta T cells rather than
525 CD4 T cells during Mycobacterium tuberculosis infection. *J. Immunol. Baltim. Md 1950*
526 2006;177(7):4662–4669.

527 42. Hu D et al. Transcriptional signature of human pro-inflammatory T H 17 cells identifies reduced
528 IL10 gene expression in multiple sclerosis. *Nat. Commun.* 2017;8(1):1600.

529 43. Chen X et al. Reduced Th17 Response in Patients with Tuberculosis Correlates with IL-6R Expression
530 on CD4+ T Cells. *Am. J. Respir. Crit. Care Med.* 2010;181(7):734–742.

531 44. Krausgruber T et al. IRF5 promotes inflammatory macrophage polarization and TH1-TH17
532 responses. *Nat. Immunol.* 2011;12(3):231–238.

533 45. Lastrucci C et al. Tuberculosis is associated with expansion of a motile, permissive and
534 immunomodulatory $CD16^+$ monocyte population via the IL-10/STAT3 axis. *Cell Res.* 2015;25(12):1333.

535 46. Rossol M, Kraus S, Pierer M, Baerwald C, Wagner U. The CD14brightCD16+ monocyte subset is
536 expanded in rheumatoid arthritis and promotes expansion of the Th17 cell population. *Arthritis*
537 *Rheum.* 2012;64(3):671–677.

538 47. Clifford V, He Y, Zufferey C, Connell T, Curtis N. Interferon gamma release assays for monitoring
539 the response to treatment for tuberculosis: A systematic review. *Tuberc. Edinb. Scotl.* 2015;95(6):639–
540 650.

541 48. Parasa VR et al. Inhibition of Tissue Matrix Metalloproteinases Interferes with Mycobacterium
542 tuberculosis-Induced Granuloma Formation and Reduces Bacterial Load in a Human Lung Tissue
543 Model [Internet]. *Front. Microbiol.* 2017;8. doi:10.3389/fmicb.2017.02370

544 49. Bray NL, Pimentel H, Melsted P, Pachter L. Near-optimal probabilistic RNA-seq quantification. *Nat.*
545 *Biotechnol.* 2016;34(5):525–527.

546 50. Soneson C, Love MI, Robinson MD. Differential analyses for RNA-seq: transcript-level estimates
547 improve gene-level inferences. *F1000Research* 2015;4:1521.

548 51. Chain B et al. Error, reproducibility and sensitivity: a pipeline for data processing of Agilent
549 oligonucleotide expression arrays. *BMC Bioinformatics* 2010;11:344.

550 52. Conesa A et al. A survey of best practices for RNA-seq data analysis. *Genome Biol.* 2016;17:13.

551 53. Breuer K et al. InnateDB: systems biology of innate immunity and beyond--recent updates and
552 continuing curation. *Nucleic Acids Res.* 2013;41(Database issue):D1228-1233.

553 54. Ricciardolo FLM et al. Identification of IL-17F/frequent exacerbator endotype in asthma. *J. Allergy*
554 *Clin. Immunol.* 2017;140(2):395–406.

555 55. Marafioti T et al. Novel markers of normal and neoplastic human plasmacytoid dendritic cells.
556 *Blood* 2008;111(7):3778–3792.

557 56. Akarca AU et al. BRAF V600E mutation-specific antibody, a sensitive diagnostic marker revealing
558 minimal residual disease in hairy cell leukaemia. *Br. J. Haematol.* 2013;162(6):848–851.

559

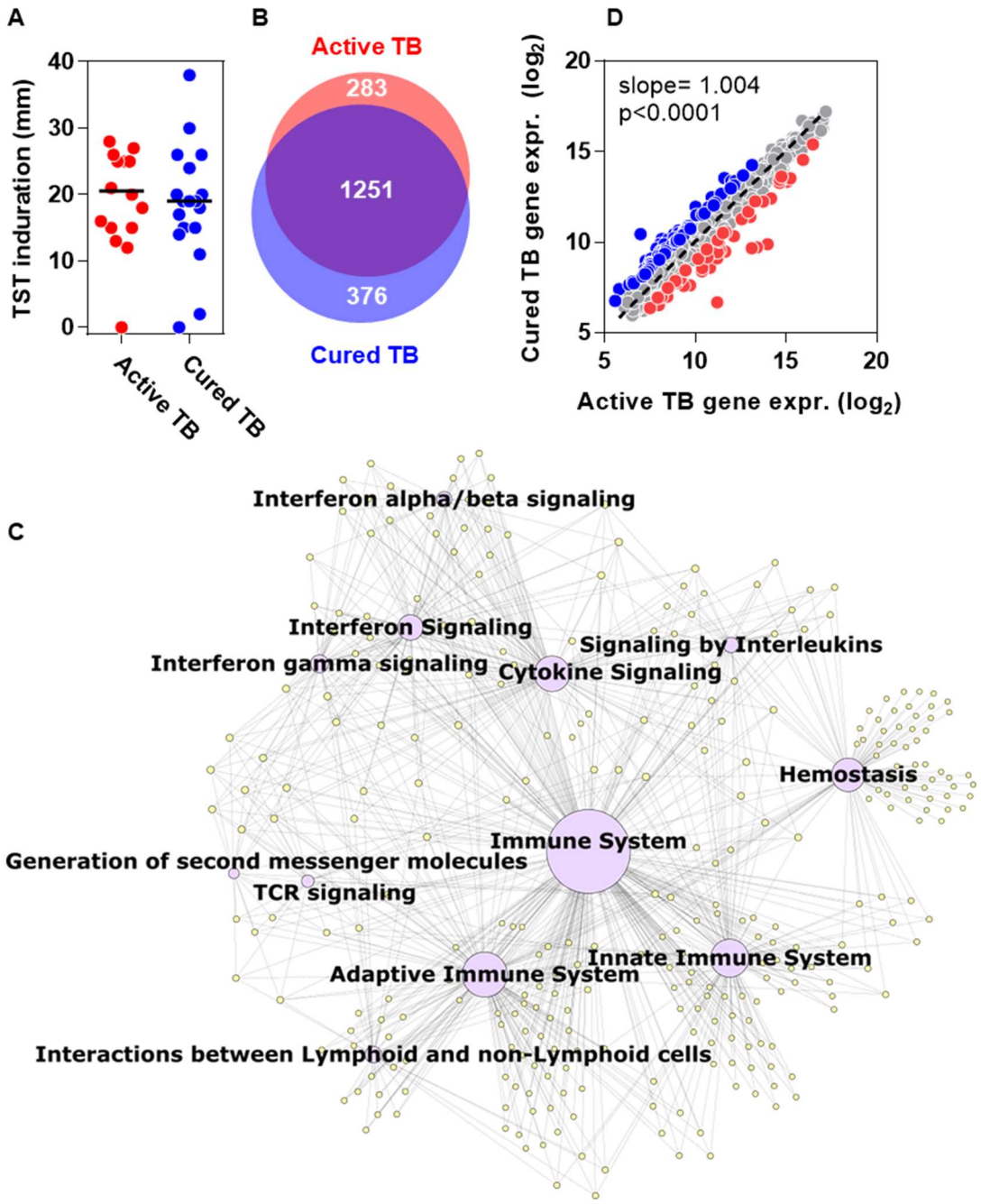

Figure 1. TST transcriptome in patients with active and cured TB disease. A) Induration at the site of TST was recorded by routine clinical assessments in both populations (mm) and was not different between the two groups (Mann-Whitney test). B) Venn diagram depicting genes significantly upregulated 2-fold in the TST of patients with active or cured TB relative to control saline injection. ($p<0.01$ by t-test with no multiple testing correction). C) TST transcriptome common to both active and cured TB summarised as a network diagram. Purple nodes represent Reactome database functional pathways, yellow nodes represent genes and edges reflect relationship between pathways and genes. Pathway node diameters are proportional to the respective pathway –log10 p value enrichment statistic. D) Pairwise dot-plot of 1910 gene integrated TST signature in patients with either active or cured TB. Dotted line reflects line of perfect covariance. p value derived from linear regression model between the two variables. Red and blue dots represent genes >2 fold differentially expressed ($p<0.01$ by t-test with no multiple testing correction) between active and cured TB.

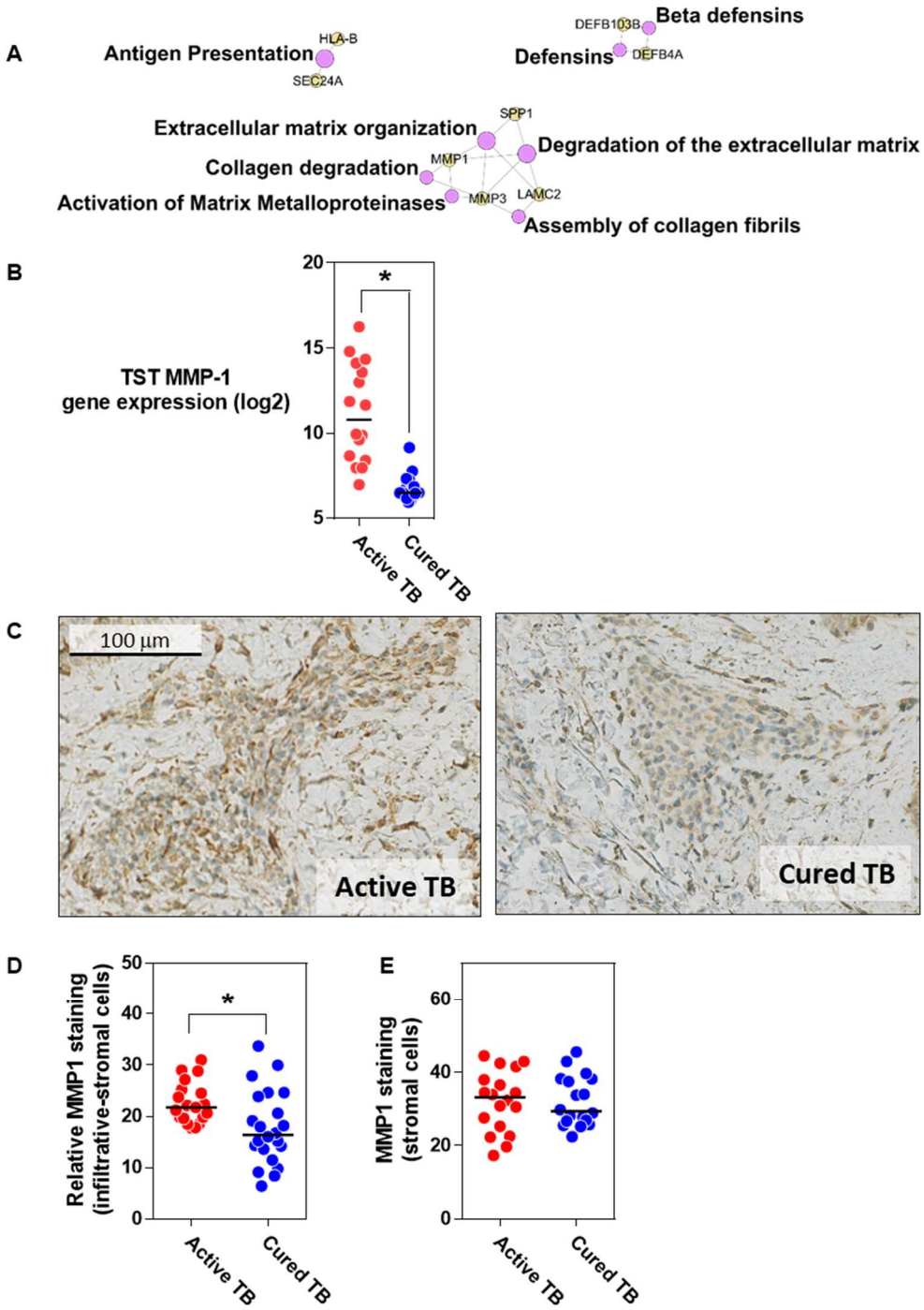

Figure 2. MMP-1 over-expression in active TB. A) Network diagram of genes and Reactome pathways over-expressed in the TST of patients with active TB compared to cured TB. Purple nodes represent Reactome database functional pathways, yellow nodes represent genes and edges reflect relationship between pathways and genes. Pathway node diameters are proportional to the respective pathway – log10 p value enrichment statistic. B) mRNA expression in TST of patients with active and cured TB of MMP1 gene. C) Representative MMP-1 immunohistochemistry staining in inflammatory infiltrates with TST samples from patients with active and cured TB. D) Differential MMP-1 staining intensity for 18 cellular infiltrates in each group of patients relative to adjacent zones of skin with no cellular infiltration. E) MMP-1 staining intensity in TST zones outside inflammatory infiltrates. * = $p<0.01$ by Mann-Whitney test.

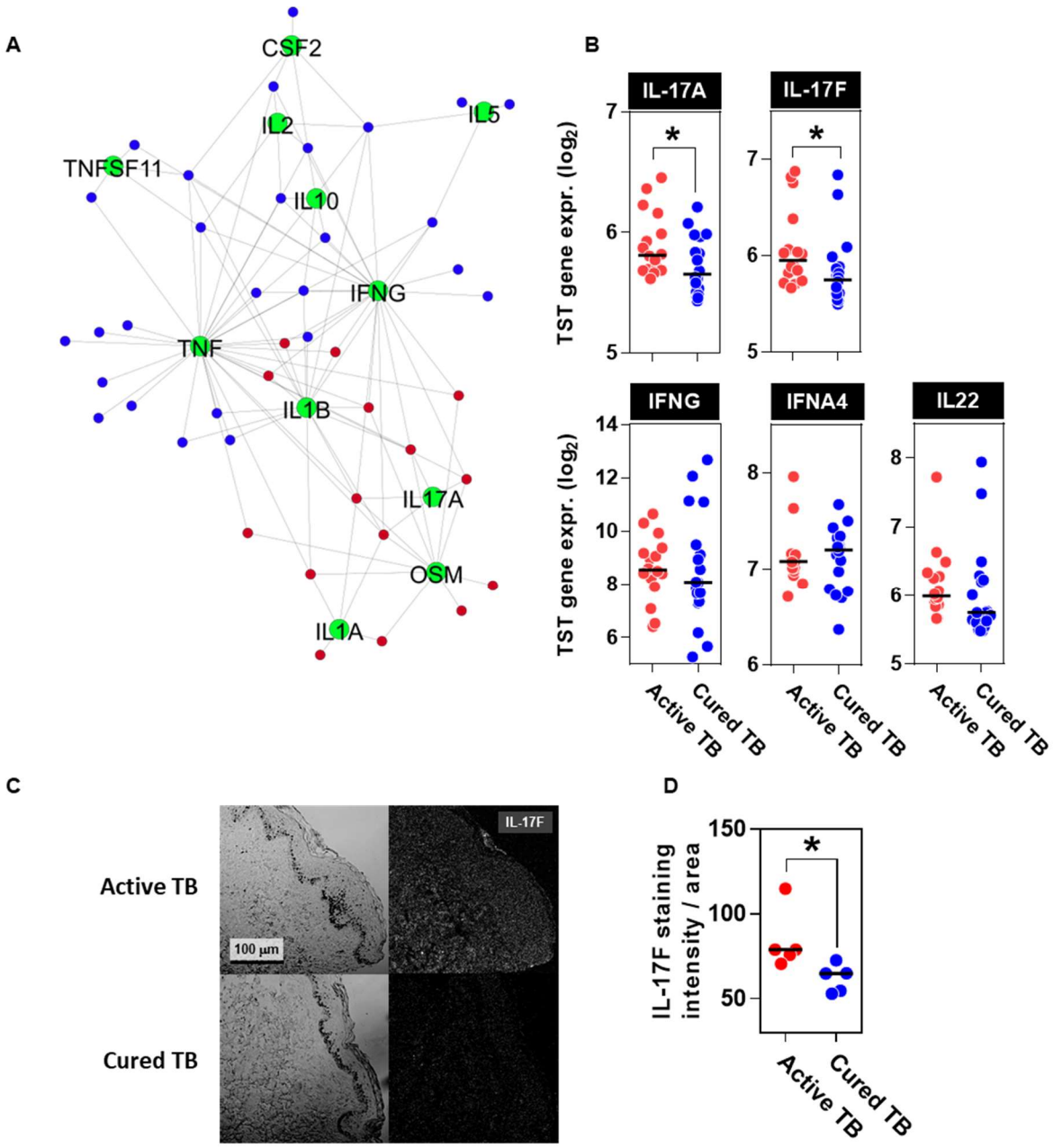

Figure 3. IL-17 is over expressed in active TB. A) Network diagram depicting upstream cytokine analysis of genes differentially expressed in TST of patients with active and cured TB. Red and blue nodes represent significant genes overexpressed in active and cured TB respectively as identified in fig 1D. Green nodes represent predicted cytokines regulating the gene expression of red and blue nodes. Edges depict relationship between upstream regulators and differentially expressed genes. B) Expression of selected cytokine transcript within the TSTs of active and cured TB patients. C) Expression of IL-17F by immunofluorescence in TST of patients with active TB. Left panel = phase contrast image, right panel = IL-17F positivity (white). D) Quantification of IL-17F staining throughout TST sections from patients with active and cured TB, determined by pixel intensity as a proportion of area sampled. Each dot represents IL-17F expression in the cross-section of an entire TST biopsy from one patient. * $p<0.01$ by Mann-Whitney test.

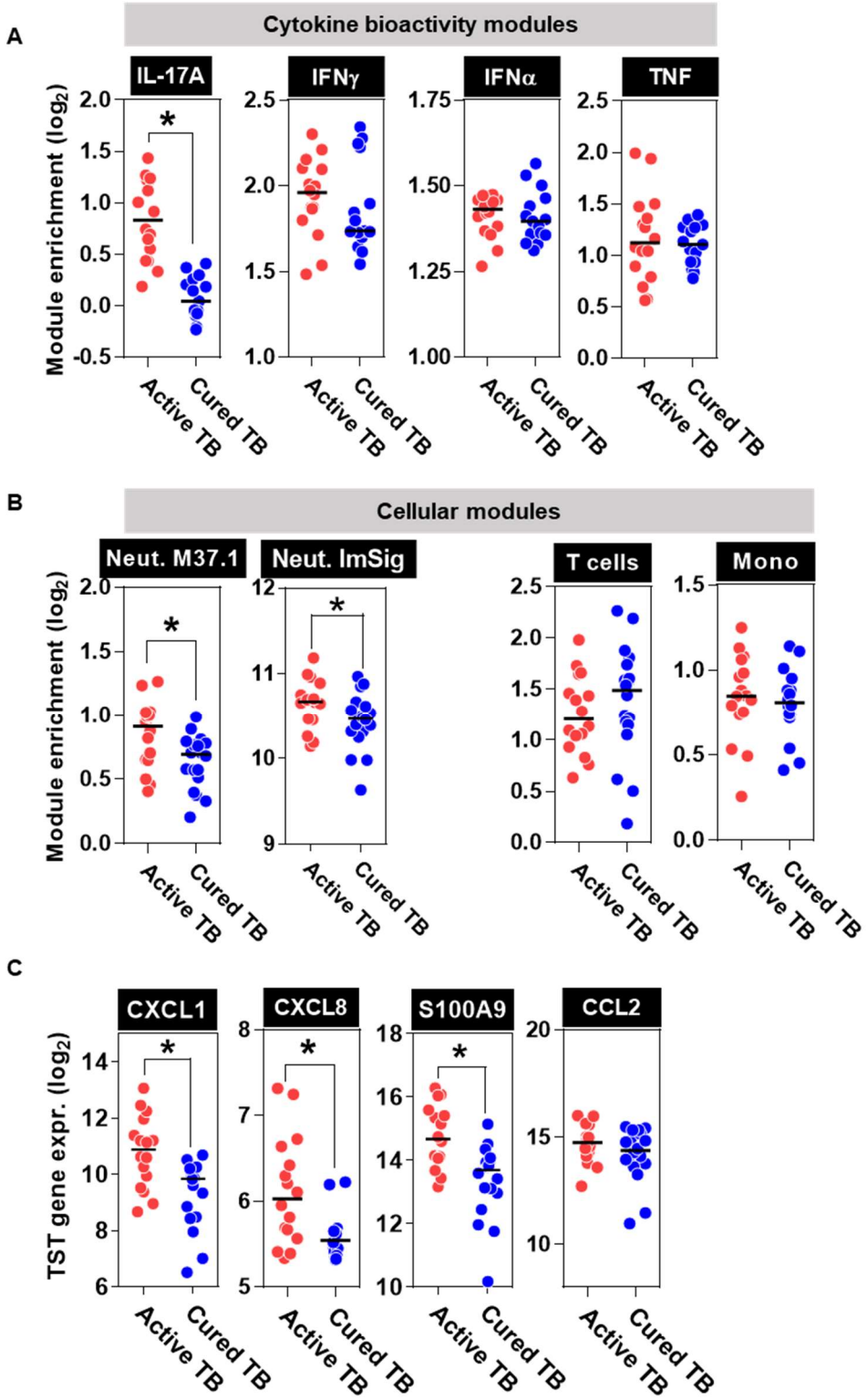

Figure 4. TST challenge in active TB is characterised by enrichment of IL-17 responses. Enrichment in TST relative to saline injection of A) keratinocyte response modules of cytokine bioactivity, B) immune cell modules and C) CXCL1, CXCL8, S100A9 and CCL2 genes. Neutrophil (Neut.) modules M37.1 and ImSig validated for sensitivity and specificity in references (23, 24) respectively. * = $p<0.01$ by Mann-Whitney test.

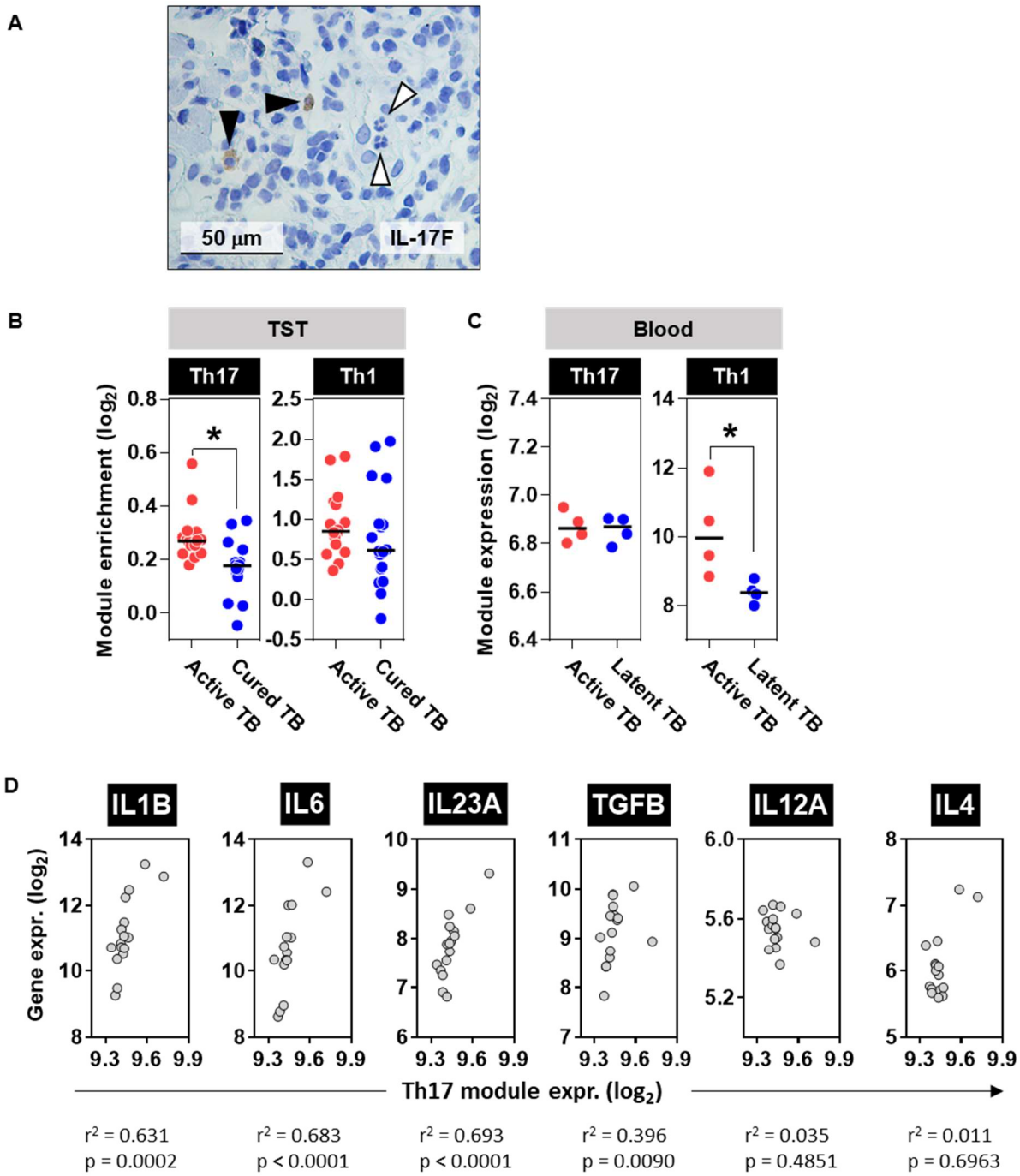

Figure 5. Active TB is characterised by elevated Th17 cells. A) IL-17F immunohistochemistry in TST of patients with active TB. Black arrows point to mononuclear cells that express IL-17F and white arrows point to polymorphonuclear cells that do not express IL-17F. B) Th17 and Th1 cell module enrichment in TST relative to saline injection. C) Expression of Th17 and Th1 modules in PPD-stimulated PBMC from patients with active or latent TB (data originated from dataset GSE27984). * = p<0.01 by Mann-Whitney test. D) Relationship between expression of Th17 transcriptional module and individual cytokine gene expression in TST of cytokines implicated in polarising CD4+ T cells to a Th17 phenotype. Data points represent patients with active TB, Spearman rank correlation coefficients (r^2) and p values.

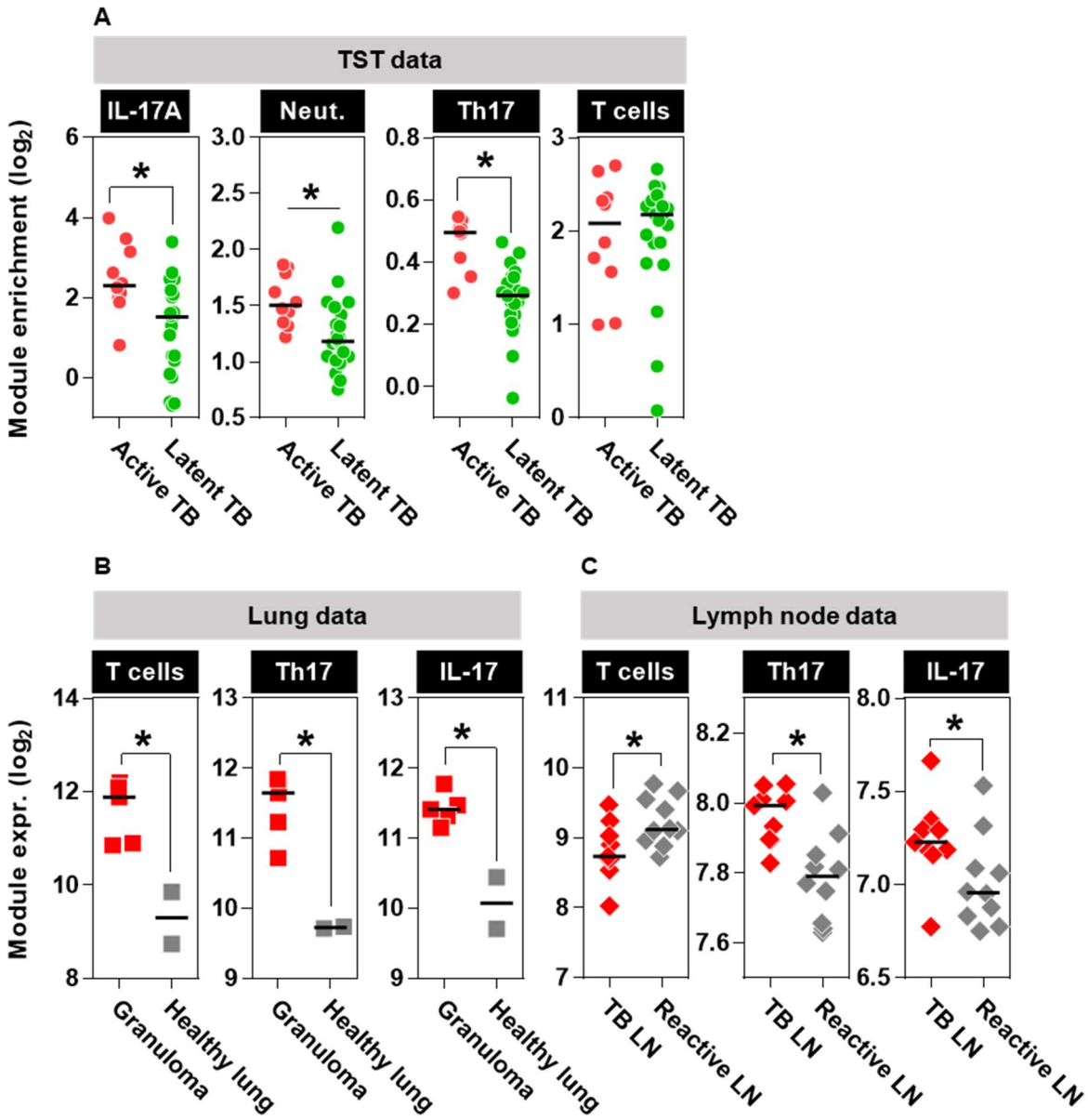

613

614 **Figure 6. Th17 cells and IL-17 activity are a feature of both TST reactions and sites of human TB**
615 **disease.** A) Enrichment in TST relative to saline injection of transcriptional modules for IL-17
616 bioactivity, neutrophils, Th17 cells and T cells in TST of independent cohort of patients with active TB
617 and a separate cohort of individuals with latent TB infection. B) Expression of T cells, Th17 cells and IL-
618 17 bioactivity modules from the site of human TB granuloma relative to healthy lung tissue (dataset
619 GSE20050) and C) in human TB infected lymph nodes (LN) relative to reactive lymph nodes that do not
620 display evidence of granulomatous inflammation or cancer (dataset E-MTAB-2547). * = $p<0.01$ by
621 Mann-Whitney test.